Peroxyl Radical Trapping Antioxidant Activity of Essential Oils and Their Phenolic Components

Wenkai Pan, Albert Velasco Abadia, Yafang Guo, Simone Gabbanini, Andrea Baschieri, Riccardo Amorati, and Luca Valgimigli

SUPPORTING INFORMATION

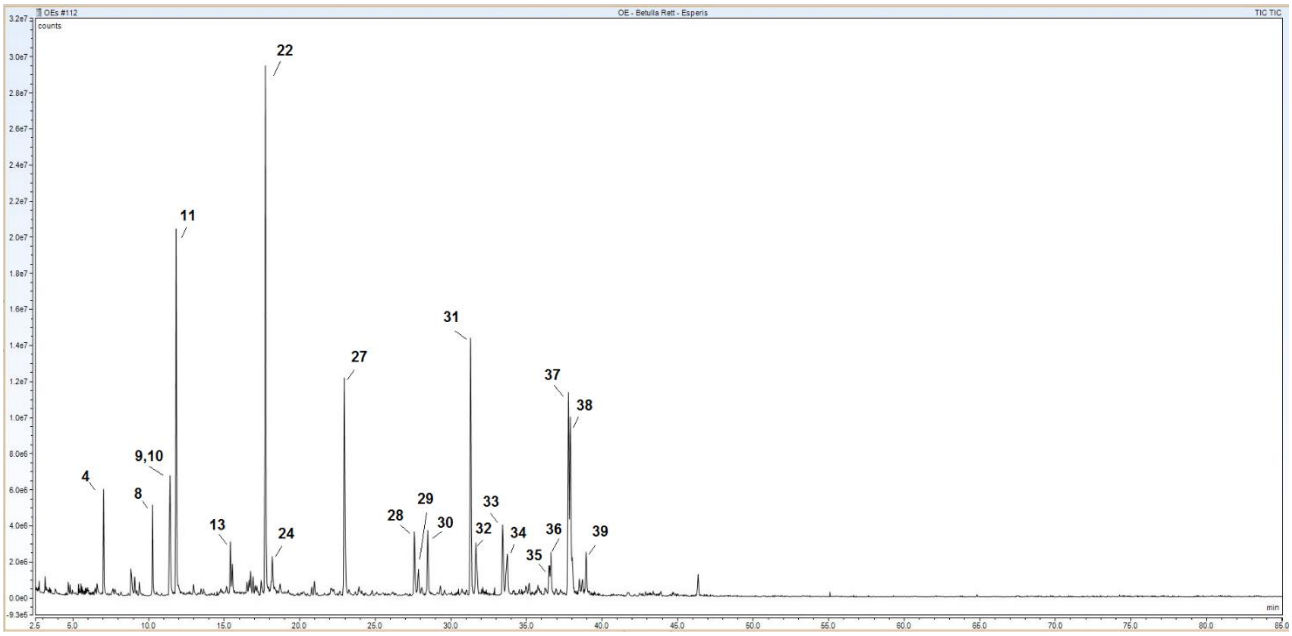

Figure S1. GC-MS (TIC in EI^+ mode at 70 EV) profile of Birch (*Betula alba*, L.) essential oil, on DB-5 column eluted with He, according to the method detailed in the manuscript. Peak numbers refer to Table S1.

Table S1. Composition of Birch (*Betula alba*, L.) essential oil, resulting from GC-MS analysis. Identification was based on Kovats retention index combined with comparison of the mass spectrum with NIST14 library. Quantitation was obtained by repeated (n=3) GC-FID injections under identical settings and reported as % area of the peak (average ± SD).

Peak #	Ret. time [min]	NIST / Kovats ID	Area %	NIST'14 r-Fit %	Kovats Index found	Kovats Index tabulated	Δ Kovats
1	3.14	2-Furaldehyde	0.16±0.01	92.3	840	835	-5
2	4.70	2-Methyl-2-cyclopentenone	0.2±0.01	98.9	908	910	2
3	4.82	Methyl 2-furyl ketone	0.15±0.01	95.9	913	913	0
4	7.02	Phenol	1.88±0.06	99.3	980	980	0
5	8.86	3-Methyl-1,2-cyclopentanedione	0.94±0.03	97.5	1023	1025	2
6	9.07	Limonene	0.36±0.01	97.5	1028	1030	2
7	9.40	2,3-dimethyl-2-cyclopentenone	0.36±0.02	94.1	1036	1040	4
8	10.26	o-Cresol	2.03±0.08	99.2	1054	1054	0
9	11.41	m-Cresol	1.45±0.02	99.1	1075	1075	0
10	11.42	p-Cresol	2.96±0.07	99.2	1076	1077	1
11	11.81	Guaiacol	8.93±0.16	99.2	1082	1087	5
12	12.96	2,6-Xylenol	0.34±0.02	94.9	1101	1108	7
13	15.40	2,5-Xylenol	1.36±0.05	99.3	1147	1151	4
14	15.53	2,4-Xylenol	0.86±0.02	98.4	1150	1152	2
15	16.51	4-Ethylphenol	0.24±0.02	96.6	1166	1169	3
16	16.64	3-Ethylphenol	0.23±0.01	99.4	1168	1169	1
17	16.73	3,5-Xylenol	0.59±0.03	97.8	1169	1171	2
18	16.90	2-Methoxy-3-methylphenol (3-methylguaiacol)	0.44±0.02	98.8	1172	1176	4
19	17.04	2,3-Dimethylphenol	0.25±0.01	95.6	1174	1177	3
20	17.15	Naphthalene	0.37±0.01	98.6	1176	1179	3

21	17.44	4-Methoxy-3-methylphenol	0.44±0.05	87.5	**1180**	1181	1
22	17.71	p-Creosol	14.73±0.43	99.1	**1184**	1190	6
23	18.09	3,4-Xylenol	0.15±0.02	96.1	**1190**	1193	3
24	18.20	1,2-Benzendiol	1.17±0.16	97.9	**1191**	1197	6
25	20.78	6-Ethyl-o-cresol	0.29±0.01	95.9	**1234**	1236	2
26	20.98	3,4-Dimethoxytoluene	0.45±0.01	96.6	**1238**	1238	0
27	22.93	Guaiacol <4-ethyl->	7.92±0.09	99.2	**1268**	1278	10
28	27.58	Pyrogallol dimethylether (Syringol)	2.10±0.06	98.7	**1342**	1350	8
29	27.85	Eugenol	1.22±0.03	91.1	**1346**	1351	5
30	28.46	Dihydroeugenol	2.07±0.07	99.5	**1356**	1368	12
31	31.30	Di-epi-α-cedrene	9.1±0.06	97.8	**1399**	1400	1
32	31.64	1,7-Dimethylnaphthalene	2.56±0.04	98.4	**1404**	1404	0
33	33.46	Dihydro-β-ionone	2.65±0.05	83.1	**1436**	1433	-3
34	33.72	Dihydrocurcumene	2.07±0.03	96.4	**1440**	1444	4
35	36.49	β-Guaiene	1.25±0.02	89.5	**1485**	1485	0
36	36.60	α-Cadinene	1.68±0.04	97.5	**1487**	1486	-1
37	37.76	β-Cadinene	6.98±0.05	95.1	**1506**	1506	0
38	37.89	Calamenene <trans->	8.4±0.12	95.3	**1508**	1508	0
39	38.95	α-Calacorene	1.39±0.03	97.8	**1527**	1529	2
40	46.33	Naphthalene, 4-isopropyl-1,6-dimethyl (Cadalene)	0.73±0.03	96.1	**1656**	1655	-1
30	28.46	Dihydroeugenol	2.07±0.05	99.5	**1356**	1368	12
31	31.30	Di-epi-α-cedrene	9.1±0.09	97.8	**1399**	1400	1
32	31.64	1,7-Dimethylnaphthalene	2.56±0.06	98.4	**1404**	1404	0
33	33.46	Dihydro-β-ionone	2.65±0.04	93.1	**1436**	1433	-3
34	33.72	Dihydrocurcumene	2.07±0.06	96.4	**1440**	1444	4
35	36.49	β-Guaiene	1.25±0.03	89.5	**1485**	1485	0
36	36.60	α-Cadinene	1.68±0.07	97.5	**1487**	1486	-1
37	37.76	β-Cadinene	6.98±0.16	95.1	**1506**	1506	0
38	37.89	Calamenene <trans->	8.4±0.14	95.3	**1508**	1508	0
39	38.95	α-Calacorene	1.39±0.05	97.8	**1527**	1529	2
40	46.33	Naphthalene, 4-isopropyl-1,6-dimethyl (Cadalene)	0.73±0.04	96.1	**1656**	1655	-1
		TOTAL IDENTIFIED	**91.45**				

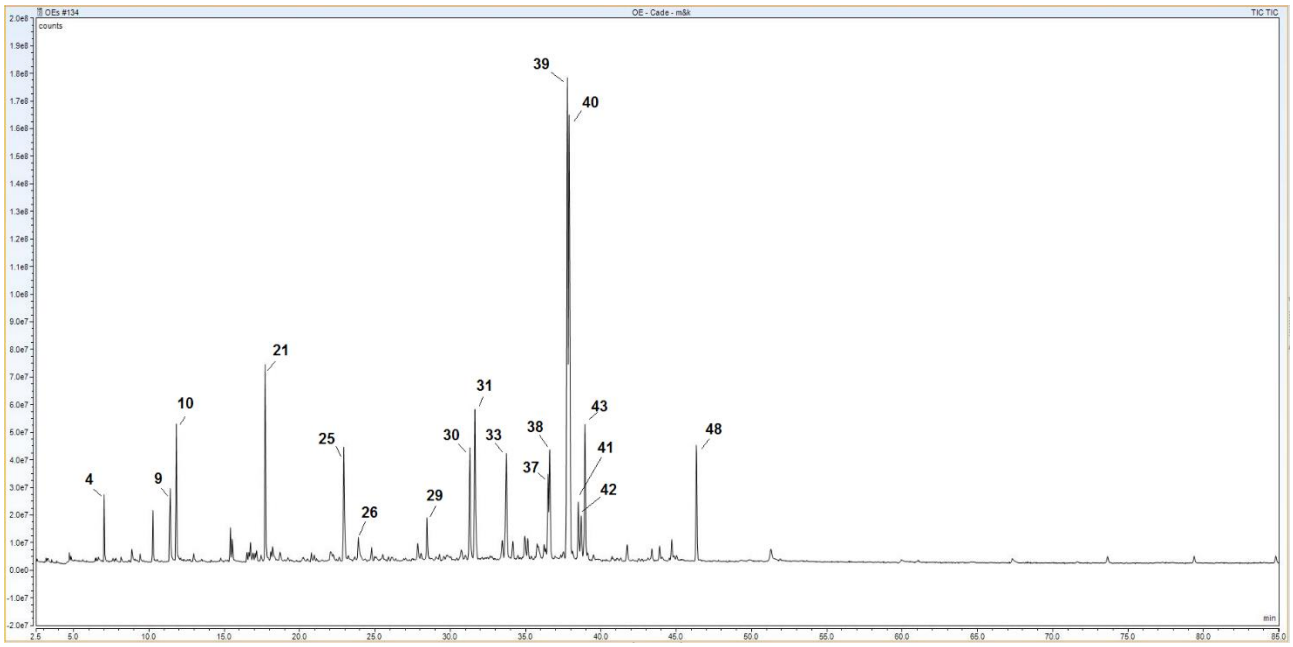

Figure S2. GC-MS (TIC in EI^+ mode at 70 EV) profile of Cade (*Juniperus oxycedrus*, L.) essential oil, on DB-5 column eluted with He, according to the method detailed in the manuscript. Peak numbers refer to Table S2.

Table S2. Composition of Cade (*Juniperus oxycedrus*, L.) essential oil, resulting from GC-MS analysis. Identification was based on Kovats retention index combined with comparison of the mass spectrum with NIST14 library. Quantitation was obtained by repeated (n=3) GC-FID injections under identical settings and reported as % area of the peak (average ± SD).

Peak #	Ret. time [min]	NIST / Kovats ID	Area %	NIST'14 r-Fit %	Kovats Index found	Kovats Index tabulated	Δ Kovats
1	3.53	α-Furfuryl alcohol	0.10±0.01	92.3	860	861	1
2	4.70	2-Methyl-2-cyclopentenone	0.13±0.01	98.9	908	910	2
3	4.82	Methyl 2-furyl ketone	0.10±0.01	95.9	913	913	0
4	7.02	Phenol	1.10±0.04	99.3	980	980	0
5	8.86	3-Methyl-1,2-cyclopentanedione	0.38±0.02	97.5	1023	1025	2
6	9.40	2,3-dimethyl-2-cyclopentenone	0.25±0.01	94.1	1036	1040	4
7	10.26	o-Cresol	0.99±0.03	99.2	1054	1054	0
8	11.41	m-Cresol	0.72±0.06	99.1	1075	1075	0
9	11.42	p-Cresol	2.34±0.10	99.2	1076	1077	1
10	11.81	Guaiacol	2.70±0.08	99.2	1082	1087	5
11	12.96	2,6-Xylenol	0.26±0.02	94.9	1101	1108	7
12	15.40	2,5-Xylenol	0.78±0.03	99.3	1147	1151	4
13	15.53	2,4-Xylenol	0.55±0.03	98.4	1150	1152	2
14	16.51	4-Ethylphenol	0.26±0.02	96.6	1166	1169	3
15	16.64	3-Ethylphenol	0.22±0.01	99.4	1168	1169	1
16	16.73	3,5-Xylenol	0.10±0.03	97.8	1169	1171	2
17	16.90	2-Methoxy-3-methylphenol	0.25±0.04	98.8	1172	1176	4
18	17.04	2,3-Dimethylphenol	0.20±0.03	95.6	1174	1177	3

19	17.15	Naphthalene	0.28±0.02	98.6	**1176**	1179	3
20	17.44	4-Methoxy-3-methylphenol	0.19±0.01	87.5	**1180**	1181	1
21	17.71	p-Creosol	5.04±0.12	99.1	**1184**	1190	6
22	18.09	3,4-Xylenol	0.27±0.04	96.1	**1190**	1193	3
23	18.20	1,2-Benzendiol	0.56±0.02	97.9	**1191**	1197	6
24	20.78	6-Ethyl-o-cresol	0.27±0.01	95.9	**1234**	1236	2
25	22.93	Guaiacol <4-ethyl->	3.68±0.09	99.2	**1268**	1278	10
26	23.89	2-Methylnaphthalene	1.14±0.05	96.1	**1282**	1288	6
27	24.78	1-Methylnaphthalene	0.42±0.02	94.2	**1295**	1297	2
28	27.85	Eugenol	0.59±0.05	91.1	**1346**	1351	5
29	28.46	Dihydroeugenol	1.32±0.07	99.5	**1356**	1368	12
30	31.30	Di-epi-α-cedrene	3.65±0.04	97.8	**1399**	1400	1
31	31.64	1,7-Dimethylnaphthalene	5.01±0.09	98.4	**1404**	1404	0
32	33.46	Dihydro-β-ionone	0.64±0.07	93.1	**1436**	1433	-3
33	33.72	Dihydrocurcumene	4.07±0.10	96.4	**1440**	1444	4
34	34.15	Cadina-3,5-diene	0.55±0.03	88.3	**1448**	1458	10
35	34.95	α-Elemene	0.86±0.04	85.2	**1461**	1462	1
36	35.13	4,5-di-epi-aristolochene	0.70±0.02	88.2	**1464**	1469	5
37	36.49	β-Guaiene	2.49±0.04	89.5	**1485**	1485	0
38	36.60	α-Cadinene	3.63±0.06	97.5	**1487**	1486	-1
39	37.76	β-Cadinene	15.74±0.72	95.1	**1506**	1506	0
40	37.89	Calamenene <trans->	16.17±1.05	95.3	**1508**	1508	0
41	38.51	Cadina-1,4-diene <trans>	1.76±0.07	93.4	**1519**	1516	-3
42	38.68	α-Dehydro-ar-himachalene	1.56±0.06	89.7	**1522**	1520	-2
43	38.95	α-Calacorene	4.50±0.08	97.8	**1527**	1529	2
44	41.75	Gleenol	0.57±0.02	94.5	**1575**	1575	0
45	43.38	Colocalene <alpha->	0.41±0.01	83.8	**1602**	1599	-3
46	43.90	Isospathulenol	0.39±0.03	88.2	**1612**	1619	7
47	44.70	Epicubenol	0.59±0.04	92.2	**1627**	1627	0
48	46.33	Naphthalene, 4-isopropyl-1,6-dimethyl (Cadalene)	3.43±0.10	96.1	**1656**	1655	-1
		TOTAL IDENTIFIED	**91.91**				

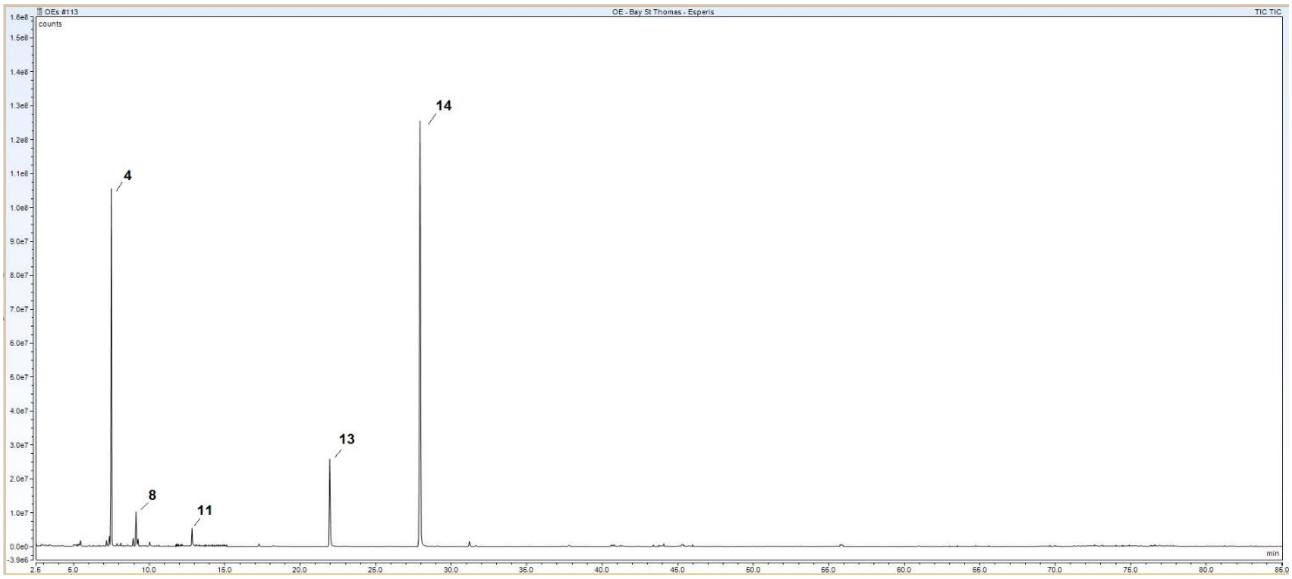

Figure S3. GC-MS (TIC in EI^+ mode at 70 EV) profile of Bay st. Thomas (*Pimenta racemosa*, Mill.) essential oil, on DB-5 column eluted with He, according to the method detailed in the manuscript. Peak numbers refer to Table S3.

Table S3. Composition of Bay st. Thomas (*Pimenta racemosa*, Mill.) essential oil, resulting from GC-MS analysis. Identification was based on Kovats retention index combined with comparison of the mass spectrum with NIST14 library. Quantitation was obtained by repeated (n=3) GC-FID injections under identical settings and reported as % area of the peak (average ± SD).

Peak #	Ret. time [min]	NIST / Kovats ID	Area %	NIST'14 r-Fit %	Kovats Index found	Kovats Index tabulated	Δ Kovats
1	5.45	α-Pinene	0.51±0.04	97.7	**936**	937	1
2	7.17	1-Octen-3-ol	0.44±0.03	99.3	**983**	982	-1
3	7.37	3-Octanone	0.59±0.03	98.1	**988**	986	-2
4	7.49	β-Myrcene	26.55±0.88	98.9	**991**	991	0
5	7.86	3-Octanol	0.19±0.01	98.2	**999**	997	-2
6	8.13	α-Phellandrene	0.28±0.01	97.7	**1005**	1005	0
7	8.94	Cymene <para->	0.59±0.02	99.1	**1025**	1025	0
8	9.13	Limonene	2.88±0.08	99.2	**1030**	1030	0
9	9.26	Eucalyptol	0.55±0.03	98.9	**1033**	1032	-1
10	10.04	trans-β-Ocimene	0.35±0.02	98.9	**1049**	1049	0
11	12.84	Linalool	1.58±0.06	98.2	**1099**	1099	0
12	17.28	Terpinen-4-ol	0.27±0.01	96.3	**1178**	1177	-1
13	21.95	p-Allylphenol (Chavicol)	8.68±0.17	99.1	**1253**	1253	0
14	27.94	Eugenol	51.25±1.04	99.4	**1348**	1351	3
15	31.20	Methyleugenol	0.64±0.03	98.6	**1397**	1402	5
		TOTAL IDENTIFIED	**95.35**				

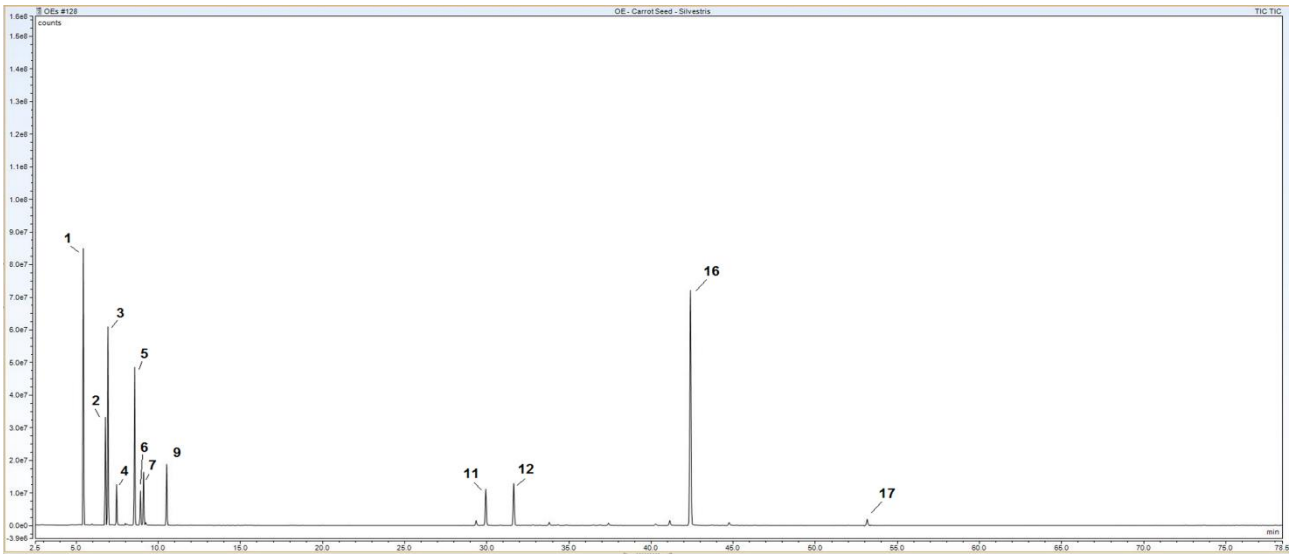

Figure S4. GC-MS (TIC in EI^+ mode at 70 EV) profile of Carrot seeds (*Daucus carota*, L.) essential oil, on DB-5 column eluted with He, according to the method detailed in the manuscript. Peak numbers refer to Table S4.

Table S4. Composition of Carrot seeds (*Daucus carota*, L.) essential oil, resulting from GC-MS analysis. Identification was based on Kovats retention index combined with comparison of the mass spectrum with NIST14 library. Quantitation was obtained by repeated (n=3) GC-FID injections under identical settings and reported as % area of the peak (average ± SD).

Peak #	Ret. time [min]	NIST / Kovats ID	Area %	NIST'14 r-Fit %	Kovats Index found	Kovats Index tabulated	Δ Kovats
1	5.43	α-Pinene	7.19±1.04	98.9	**935**	937	2
2	6.77	Sabinene	7.10±0.12	99.3	**973**	974	1
3	6.93	β-Pinene	13.41±0.42	99.4	**977**	978	1
4	7.46	β-Myrcene	2.72±0.13	99.2	**990**	991	1
5	8.55	α-Terpinene	11.11±0.40	99.3	**1016**	1017	1
6	8.90	p-Cymene	2.32±0.09	99.1	**1024**	1025	1
7	9.10	Limonene	3.85±0.08	99.2	**1029**	1031	2
8	9.23	Eucalyptol	0.19±0.01	98.6	**1032**	1032	0
9	10.50	γ-Terpinene	4.39±0.14	98.8	**1059**	1060	1
10	29.35	Daucene	0.55±0.02	97.7	**1370**	1376	6
11	29.93	Geranyl acetate	3.55±0.07	98.3	**1378**	1379	1
12	31.63	β-cis-Caryophyllene	4.4±0.09	98.4	**1404**	1406	2
13	33.79	Humulene	0.35±0.02	90.2	**1442**	1446	4
14	37.38	cis-α-Bisabolene	0.27±0.01	96.5	**1499**	1500	1
15	41.14	β-Caryophyllene oxide	0.56±0.03	92.8	**1565**	1567	2
16	42.40	Carotol	26.65±1.10	98.1	**1586**	1592	6
17	53.24	Umbelliferone	0.86±0.04	92.0	**1784**	1789	5
		TOTAL IDENTIFIED	**99.47**				

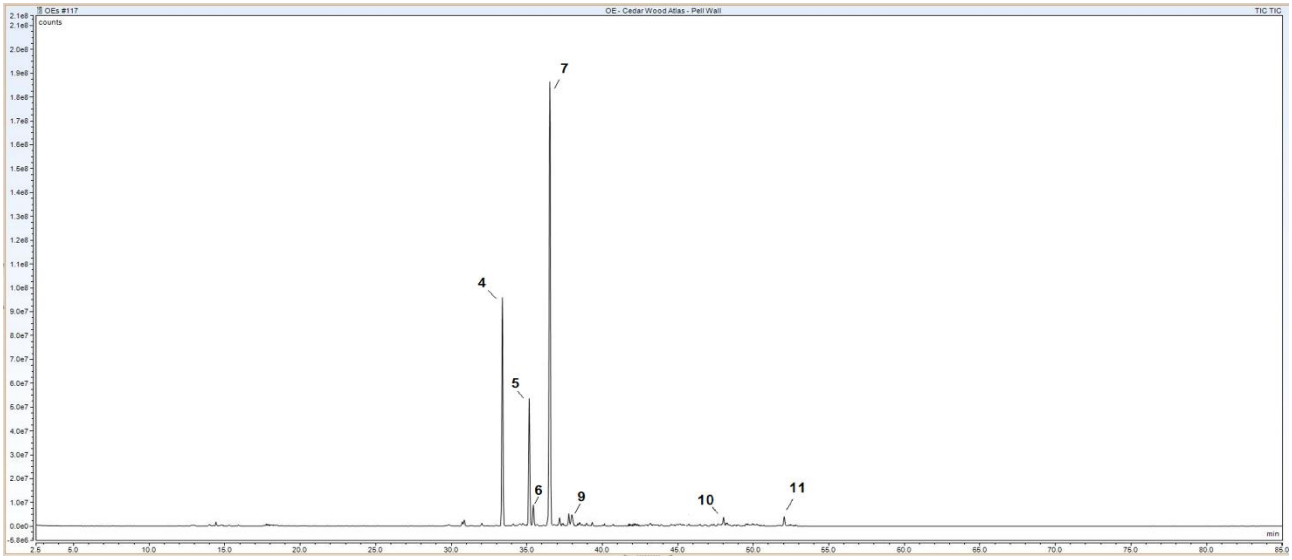

Figure S5. GC-MS (TIC in EI^+ mode at 70 EV) profile of Cedarwood Atlas (*Cupressus atlantica,* Gaussen) essential oil, on DB-5 column eluted with He, according to the method detailed in the manuscript. Peak numbers refer to Table S5.

Table S5. Composition of Cedarwood Atlas (*Cupressus atlantica,* Gaussen) essential oil, resulting from GC-MS analysis. Identification was based on Kovats retention index combined with comparison of the mass spectrum with NIST14 library. Quantitation was obtained by repeated (n=3) GC-FID injections Cedarwood Atlas (*Cupressus atlantica, Gaussen*) under identical settings and reported as % area of the peak (average ± SD).

Peak #	Ret. time [min]	NIST / Kovats ID	Area %	NIST'14 r-Fit %	Kovats Index found	Kovats Index tabulated	Δ Kovats
1	14.42	Limona ketone	0.29±0.01	96.6	**1130**	1131	1
2	30.73	Isolongipholene	0.38±0.01	87.5	**1390**	1390	0
3	30.86	Longifolene	0.59±0.02	98.5	**1392**	1394	2
4	33.38	Thujopsene	22.91±0.20	94.1	**1435**	1435	0
5	35.16	Alloaromadendrene	12.38±0.17	91.8	**1464**	1464	0
6	35.43	Himachala-2,4-diene	1.93±0.06	93.8	**1468**	1462	-6
7	36.53	β-Himachalene	49.22±1.22	90.4	**1486**	1494	8
8	37.17	α-Dehydro-ar-himachalene	0.82±0.04	96.7	**1496**	1512	16
9	37.78	Bicyclo[4.4.0]dec-1-ene, 2-isopropyl-5-methyl-9-methylene-	1.07±0.08	88.8	**1506**	1507	1
10	47.79	(E)-Coniferyl alcohol	0.88±0.07	93.4	**1686**	1689	3
11	52.04	(E)-Atlantone	1.13±0.08	95.7	**1761**	1769	8
		TOTAL IDENTIFIED	**91.60**				

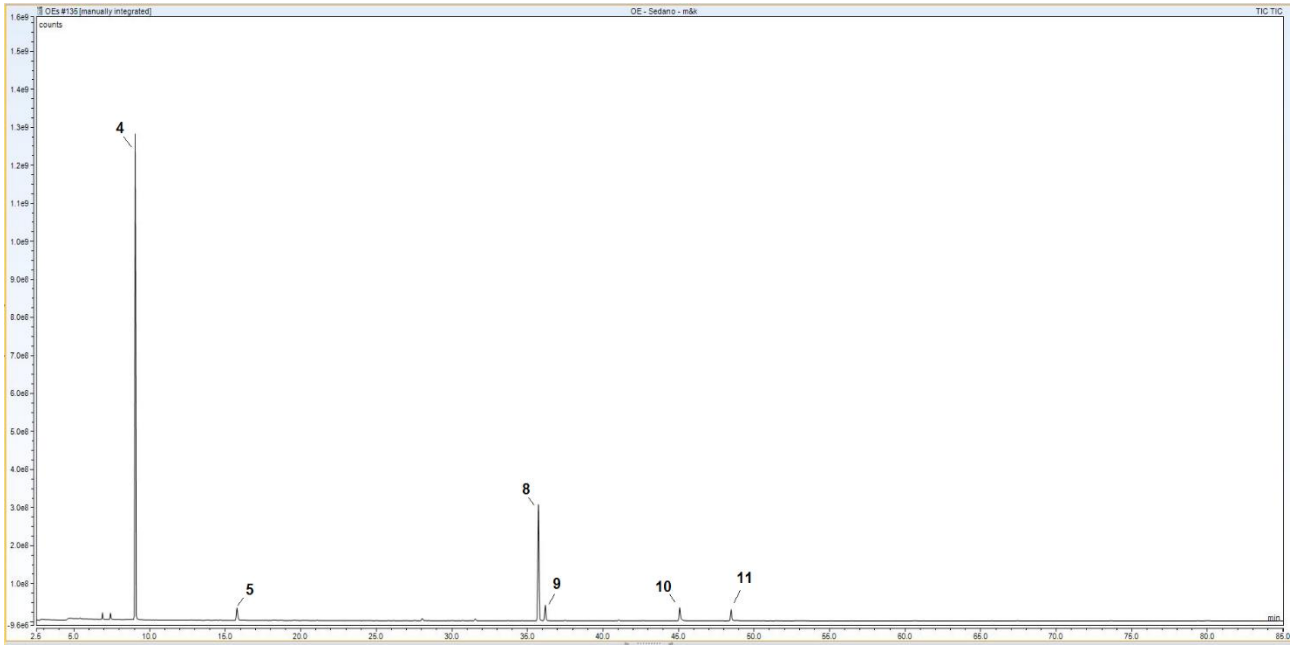

Figure S6. GC-MS (TIC in EI^+ mode at 70 EV) profile of Celery *(Apium graveolens,* L.) essential oil, on DB-5 column eluted with He, according to the method detailed in the manuscript. Peak numbers refer to Table S6.

Table S6. Composition of Celery *(Apium graveolens,* L.) essential oil, resulting from GC-MS analysis. Identification was based on Kovats retention index combined with comparison of the mass spectrum with NIST14 library. Quantitation was obtained by repeated (n=3) GC-FID injections under identical settings and reported as % area of the peak (average ± SD).

Peak #	Ret. time [min]	NIST / Kovats ID	Area %	NIST'14 r-Fit %	Kovats Index found	Kovats Index tabulated	Δ Kovats
1	5.45	α-Pinene	0.14±0.01	98.9	936	937	1
2	6.95	β-Pinene	0.78±0.02	99.2	978	978	0
3	7.49	β-Myrcene	0.75±0.03	98.9	991	991	0
4	9.13	Limonene	64.65±2.04	99.2	1030	1031	1
5	15.85	Pentylbenzene	2.35±0.08	99.2	1155	1157	2
6	28.34	Valerophenone	0.43±0.02	98.3	1354	1359	5
7	31.71	β-cis-Caryophyllene	0.37±0.02	98.4	1406	1406	0
8	35.73	β-Selinene	20.62±0.56	99.1	1485	1485	0
9	36.19	Selinene <alpha->	2.6±0.12	97.8	1493	1494	1
10	45.18	3-Butylphthalide	2.77±0.08	98.7	1651	1656	5
11	48.48	Sedanenolide	2.19±0.10	93.4	1734	1735	1
		TOTAL IDENTIFIED	**97.65**				

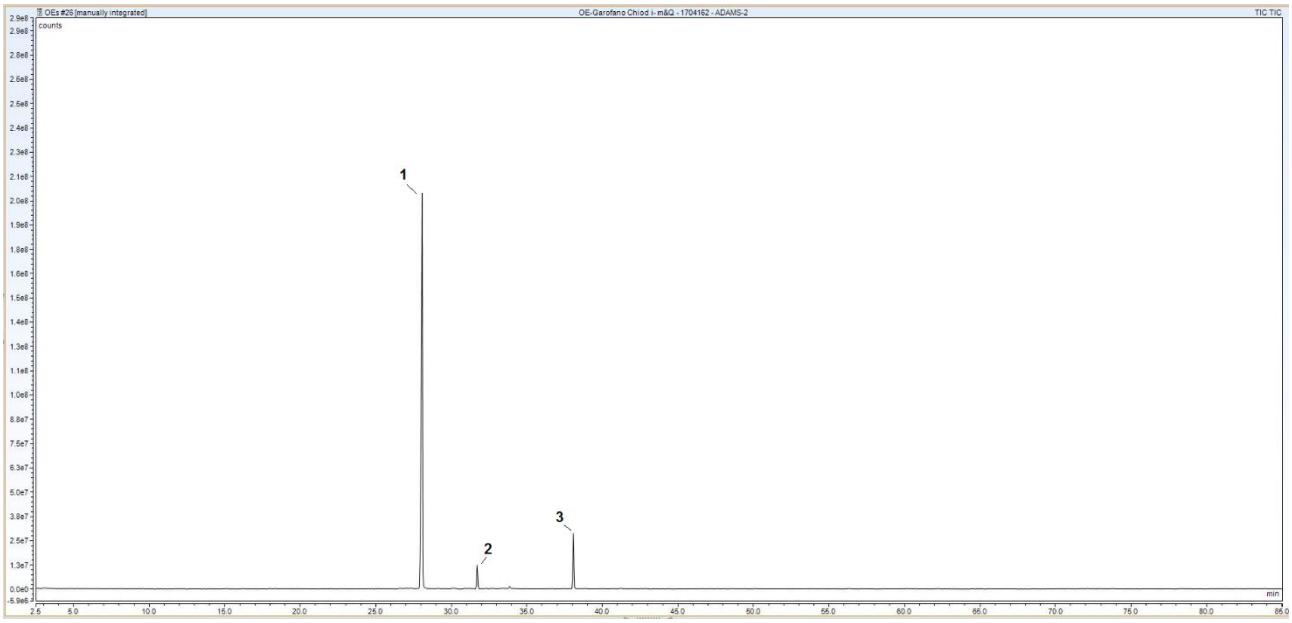

Figure S7. GC-MS (TIC in EI^+ mode at 70 EV) profile of Clove bud 1 (*Syzygium aromaticum,* L.) essential oil, on DB-5 column eluted with He, according to the method detailed in the manuscript. Peak numbers refer to Table S7.

Table S7. Composition of Clove bud 1 (*Syzygium aromaticum,* L.) essential oil, resulting from GC-MS analysis. Identification was based on Kovats retention index combined with comparison of the mass spectrum with NIST14 library. Quantitation was obtained by repeated (n=3) GC-FID injections under identical settings and reported as % area of the peak (average ± SD).

Peak #	Ret. time [min]	NIST / Kovats ID	Area %	NIST'14 r-Fit %	Kovats Index found	Kovats Index tabulated	Δ Kovats
1	28.08	Eugenol	86.02±1.72	98.3	1350	1351	1
2	31.72	β-cis-Caryophyllene	4.24±0.09	98.4	1406	1406	0
3	38.08	Eugenyl acetate	9.37±0.34	98.6	1511	1522	11
		TOTAL IDENTIFIED	**99.63**				

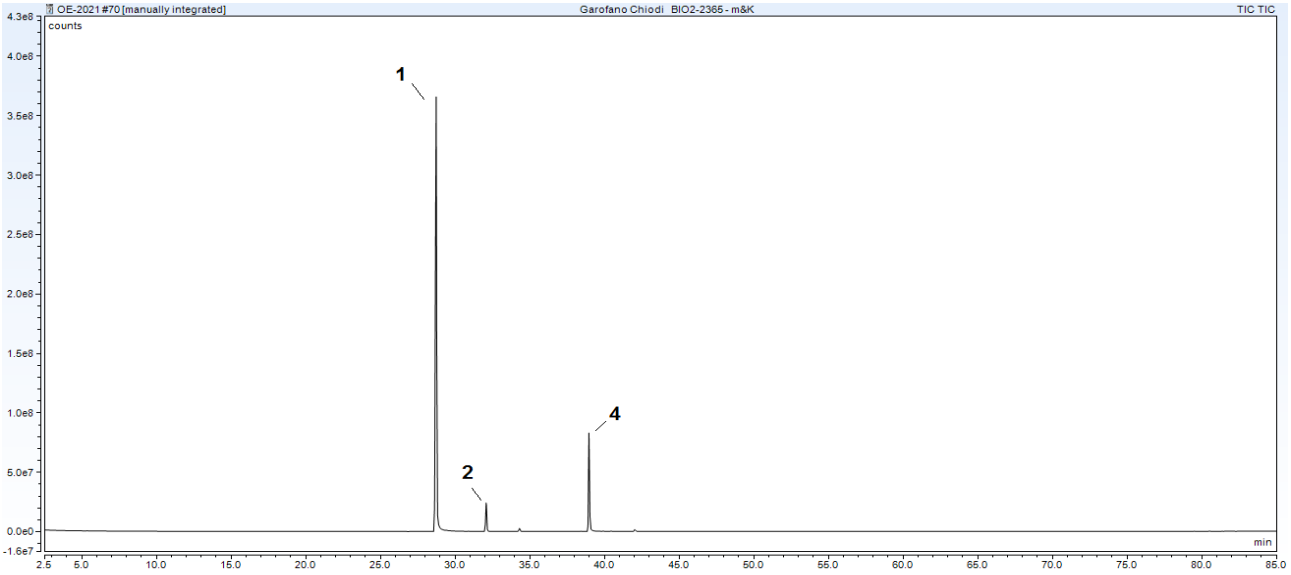

Figure S8. GC-MS (TIC in EI^+ mode at 70 EV) profile of Clove bud 2 (*Syzygium aromaticum,* L.) essential oil, on DB-5 column eluted with He, according to the method detailed in the manuscript. Peak numbers refer to Table S8.

Table S8. Composition of Clove bud 2 (*Syzygium aromaticum,* L.) essential oil, resulting from GC-MS analysis. Identification was based on Kovats retention index combined with comparison of the mass spectrum with NIST14 library. Quantitation was obtained by repeated (n=3) GC-FID injections under identical settings and reported as % area of the peak (average ± SD).

Peak #	Ret. time [min]	NIST / Kovats ID	Area %	NIST'14 r-Fit %	Kovats Index found	Kovats Index tabulated	Δ Kovats
1	28.08	Eugenol	73.90±1.54	99.6	1350	1351	1
2	32.08	β-cis-Caryophyllene	4.63±0.14	98.4	1406	1406	0
3	34.31	α-Humulene	0.48±0.02	96.3	1454	1454	0
4	38.96	Eugenyl acetate	15.83±0.48	98.6	1511	1522	11
5	42.04	Caryophyllene oxide	0.38±0.02	97.2	1574	1574	0
		TOTAL IDENTIFIED	**95.92**				

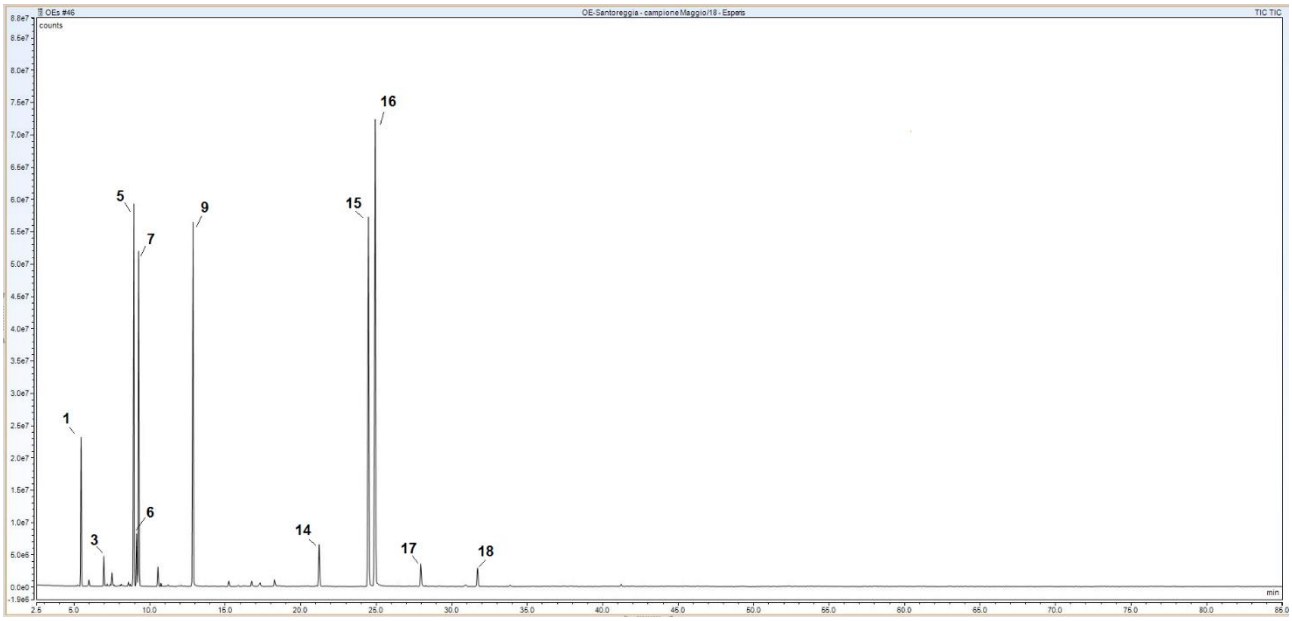

Figure S9. GC-MS (TIC in EI^+ mode at 70 EV) profile of Winter Savory (*Satureja montana*, L.) essential oil, on DB-5 column eluted with He, according to the method detailed in the manuscript. Peak numbers refer to Table S9.

Table S9. Composition of Winter Savory (*Satureja montana*, L.) essential oil, resulting from GC-MS analysis. Identification was based on Kovats retention index combined with comparison of the mass spectrum with NIST14 library. Quantitation was obtained by repeated (n=3) GC-FID injections under identical settings and reported as % area of the peak (average ± SD).

Peak #	Ret. time [min]	NIST / Kovats ID	Area %	NIST'14 r-Fit %	Kovats Index found	Kovats Index tabulated	Δ Kovats
1	5.43	α-Pinene	5.62±0.18	98.9	**935**	937	2
2	5.97	Camphene	0.28±0.01	98.3	**952**	951	-1
3	6.95	β-Pinene	1.13±0.05	99.2	**978**	978	0
4	7.49	β-Myrcene	0.54±0.04	98.9	**991**	991	0
5	8.94	p-Cymene	13.86±0.36	99.1	**1025**	1025	0
6	9.13	Limonene	1.86±0.10	99.2	**1030**	1031	1
7	9.26	Eucalyptol	12.03±0.15	98.6	**1033**	1032	-1
8	10.54	γ-Terpinene	0.75±0.07	98.8	**1059**	1060	1
9	12.86	Linalool	15.08±0.40	99.3	**1100**	1099	-1
10	15.24	Camphor	0.24±0.01	99.2	**1145**	1145	0
11	16.75	Borneol	0.33±0.03	98.4	**1169**	1168	-1
12	17.31	Terpinen-4-ol	0.28±0.01	98.3	**1178**	1177	-1
13	18.26	α-Terpineol	0.38±0.02	99.4	**1192**	1190	-2
14	21.22	Carvone	2.12±0.11	98.2	**1241**	1242	1
15	24.48	Thymol	18.70±0.41	97.8	**1291**	1291	0
16	24.93	Carvacrol	23.51±0.55	98.2	**1297**	1299	2
17	27.94	Eugenol	1.23±0.05	98.3	**1348**	1351	3
18	31.71	β-cis-Caryophyllene	1.09±0.06	98.4	**1406**	1406	0
		TOTAL IDENTIFIED	**99.03**				

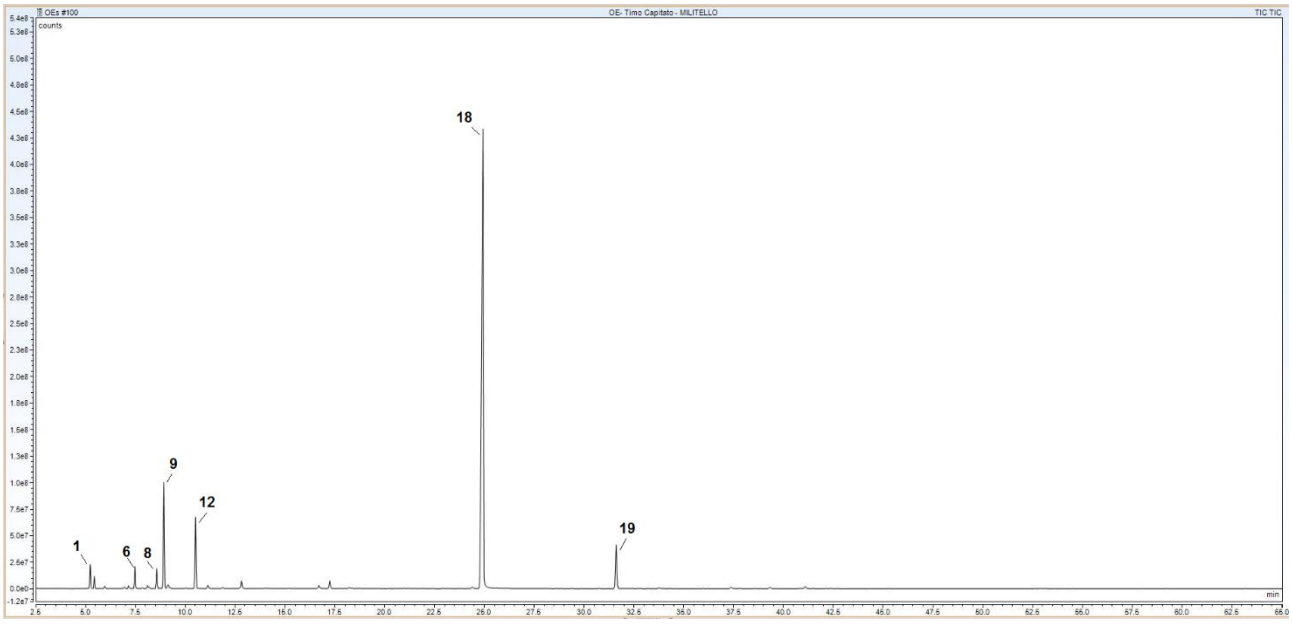

Figure S10. GC-MS (TIC in EI$^+$ mode at 70 EV) profile of Spanish Oregano (*Thymbra capitata,* L., Cav.) essential oil, on DB-5 column eluted with He, according to the method detailed in the manuscript. Peak numbers refer to Table S10.

Table S10. Composition of Spanish Oregano (*Thymbra capitata,* L., Cav.) essential oil, resulting from GC-MS analysis. Identification was based on Kovats retention index combined with comparison of the mass spectrum with NIST14 library. Quantitation was obtained by repeated (n=3) GC-FID injections under identical settings and reported as % area of the peak (average ± SD).

Peak #	Ret. time [min]	NIST / Kovats ID	Area %	NIST'14 r-Fit %	Kovats Index found	Kovats Index tabulated	Δ Kovats
1	5.22	α-Thujene	1.59±0.11	99.1	928	929	1
2	5.43	α-Pinene	0.81±0.03	99.6	935	937	2
3	5.97	Camphene	0.18±0.01	98.3	952	951	-1
4	6.95	β-Pinene	0.15±0.01	99.2	978	978	0
5	7.15	1-Octen-3-ol	0.23±0.02	98.9	983	982	-1
6	7.47	β-Myrcene	1.57±0.07	98.9	990	991	1
7	8.10	α-Phellandrene	0.24±0.01	97.5	1005	1005	0
8	8.56	α-Terpinen	1.52±0.06	99.1	1016	1017	1
9	8.92	p-Cymene	8.15±0.41	99.1	1025	1025	0
10	9.11	Limonene	0.26±0.01	99.2	1029	1031	2
11	9.15	Phellandrene <beta->	0.24±0.01	97.9	1030	1030	0
12	10.51	γ-Terpinene	5.87±0.23	98.8	1059	1060	1
13	11.13	cis-Sabinenhydrate	0.29±0.01	97.8	1070	1070	0
14	12.81	Linalool	0.76±0.04	99.3	1099	1099	0
15	16.70	Borneol	0.35±0.02	98.4	1169	1168	-1
16	17.24	Terpinen-4-ol	0.76±0.12	98.3	1177	1177	0
17	18.21	α-Terpineol	0.13±0.01	99.4	1191	1190	-1
18	24.93	Carvacrol	69.43±1.19	98.2	1297	1299	2
19	31.61	β-cis-Caryophyllene	5.12±0.12	98.4	1404	1406	2
		TOTAL IDENTIFIED	**97.65**				

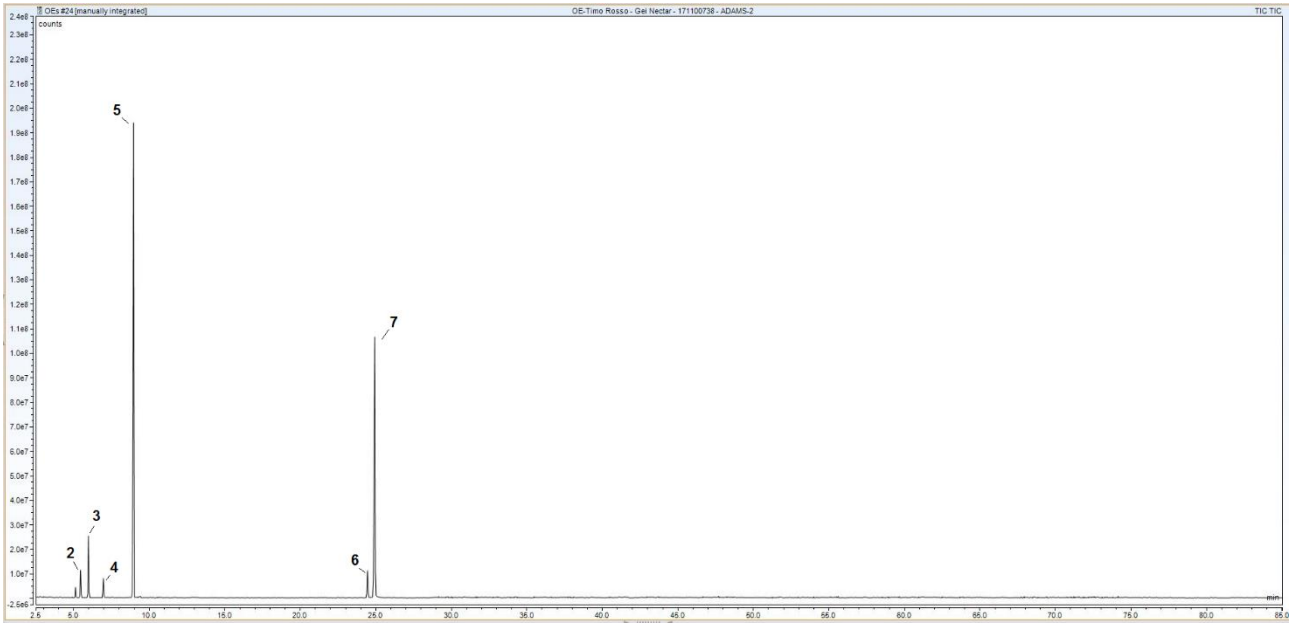

Figure S11. GC-MS (TIC in EI^+ mode at 70 EV) profile of Red Thyme 1 (*Thymus vulgaris*, L.) essential oil, on DB-5 column eluted with He, according to the method detailed in the manuscript. Peak numbers refer to Table S11.

Table S11. Composition of Red Thyme 1 (*Thymus vulgaris*, L.) essential oil, resulting from GC-MS analysis. Identification was based on Kovats retention index combined with comparison of the mass spectrum with NIST14 library. Quantitation was obtained by repeated (n=3) GC-FID injections under identical settings and reported as % area of the peak (average ± SD).

Peak #	Ret. time [min]	NIST / Kovats ID	Area %	NIST'14 r-Fit %	Kovats Index found	Kovats Index tabulated	Δ Kovats
1	5.12	Tricyclene	0.96±0.03	98.9	924	925	1
2	5.46	α-Pinene	2.65±0.08	99.6	936	937	1
3	5.98	Camphene	6.16±0.12	99.2	952	951	-1
4	6.96	β-Pinene	1.95±0.07	99.2	978	978	0
5	8.96	p-Cymene	43.43±0.74	99.1	1026	1025	-1
6	24.45	Thymol	3.44±0.08	99.4	1290	1291	1
7	24.93	Carvacrol	36.39±0.42	98.2	1297	1299	2
		TOTAL IDENTIFIED	**94.98**				

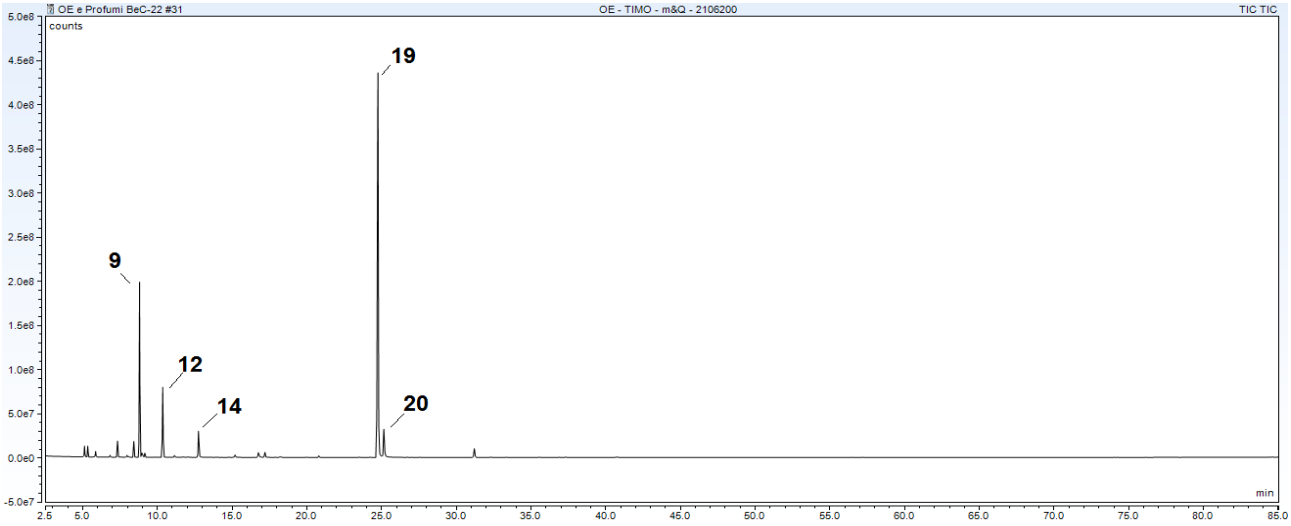

Figure S12. GC-MS (TIC in EI^+ mode at 70 EV) profile of Red Thyme 2 (*Thymus vulgaris*, L.) essential oil, on DB-5 column eluted with He, according to the method detailed in the manuscript. Peak numbers refer to Table S12.

Table S12. Composition of Red Thyme 2 (*Thymus vulgaris*, L.) essential oil, resulting from GC-MS analysis. Identification was based on Kovats retention index combined with comparison of the mass spectrum with NIST14 library. Quantitation was obtained by repeated (n=3) GC-FID injections under identical settings and reported as % area of the peak (average ± SD).

Peak #	Ret. time [min]	NIST / Kovats ID	Area %	NIST'14 r-Fit %	Kovats Index found	Kovats Index tabulated	Δ Kovats
1	5.12	Tricyclene	0.85±0.05	98.9	924	925	1
2	5.46	α-Pinene	0.90±0.04	99.6	936	937	1
3	5.96	Camphene	0.51±0.04	99.2	952	951	-1
4	6.83	β-Pinene	0.18±0.01	99.2	978	978	0
5	7.33	β-Myrcene	1.43±0.05	99.2	991	991	0
6	7.96	α-Phellandrene	0.17±0.01	98.5	1005	1005	0
7	8.06	δ 3-carene	0.10±0.01	97.9	1011	1011	0
8	8.42	Terpinene	1.51±0.04	98.2	1016	1016	0
9	8.85	p-Cymene	16.36±0.12	99.1	1026	1025	-1
10	8.97	Limonene	0.48±0.02	96.7	1029	1029	0
11	9.16	1,8-Cineole	0.41±0.01	98.2	1032	1032	0
12	10.36	γ-Terpinene	7.2±0.11	99.4	1060	1060	0
13	11.13	cis-Sabinene hydrate	0.28±0.01	98.3	1070	1070	0
14	12.75	Linalool	3.19±0.14	99.4	1099	1099	0
15	15.19	Camphor	0.30±0.02	99.2	1142	1142	0
16	16.75	Borneol	0.83±0.04	98.1	1167	1168	1
17	17.19	Terpinen-4-ol	0.76±0.03	98.2	1177	1177	0
18	20.80	Thymol methyl ether	0.24±0.01	98.7	1235	1235	0
19	24.76	Thymol	53.77±0.88	99.4	1290	1291	1
20	25.15	Carvacrol	3.50±0.06	98.9	1297	1296	-1
21	31.21	Cariofillene	1.34±0.04	99.3	1404	1404	0
		TOTAL IDENTIFIED	**97.83**				

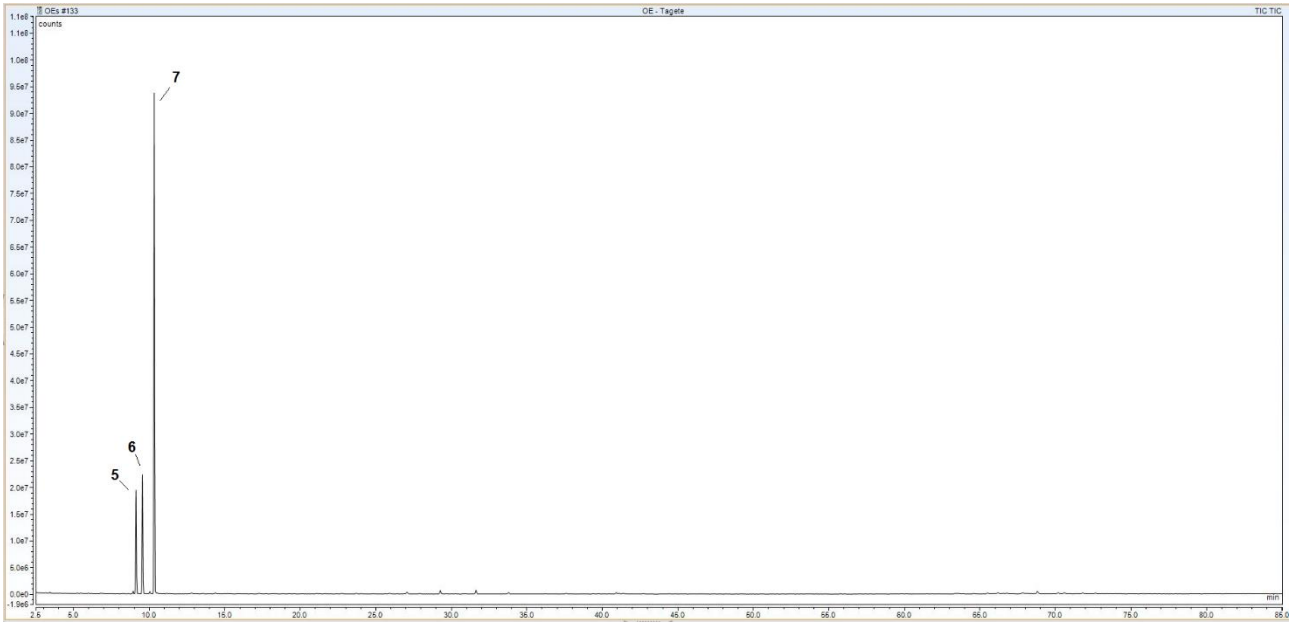

Figure S13. GC-MS (TIC in EI^+ mode at 70 EV) profile of Wild Marigold (*Tagetes minuta*, L.) essential oil, on DB-5 column eluted with He, according to the method detailed in the manuscript. Peak numbers refer to Table S13.

Table S13. Composition of Wild Marigold (*Tagetes minuta*, L.) essential oil, resulting from GC-MS analysis. Identification was based on Kovats retention index combined with comparison of the mass spectrum with NIST14 library. Quantitation was obtained by repeated (n=3) GC-FID injections under identical settings and reported as % area of the peak (average ± SD).

Peak #	Ret. time [min]	NIST / Kovats ID	Area %	NIST'14 r-Fit %	Kovats Index found	Kovats Index tabulated	Δ Kovats
1	5.22	α-Thujene	0.14±0.01	99.1	928	929	1
2	5.43	α-Pinene	0.15±0.01	98.9	935	937	2
3	6.81	Sabinen	0.19±0.01	99.2	974	974	0
4	8.94	p-Cymene	0.35±0.03	97.5	1025	1025	0
5	9.13	Limonene	13.18±0.36	99.2	1030	1031	1
6	9.55	β-cis-Ocimene	14.53±0.43	99.6	1039	1039	0
7	10.33	Dihydrotagetone	63.57±1.42	99.5	1055	1059	4
		TOTAL IDENTIFIED	**92.11**				

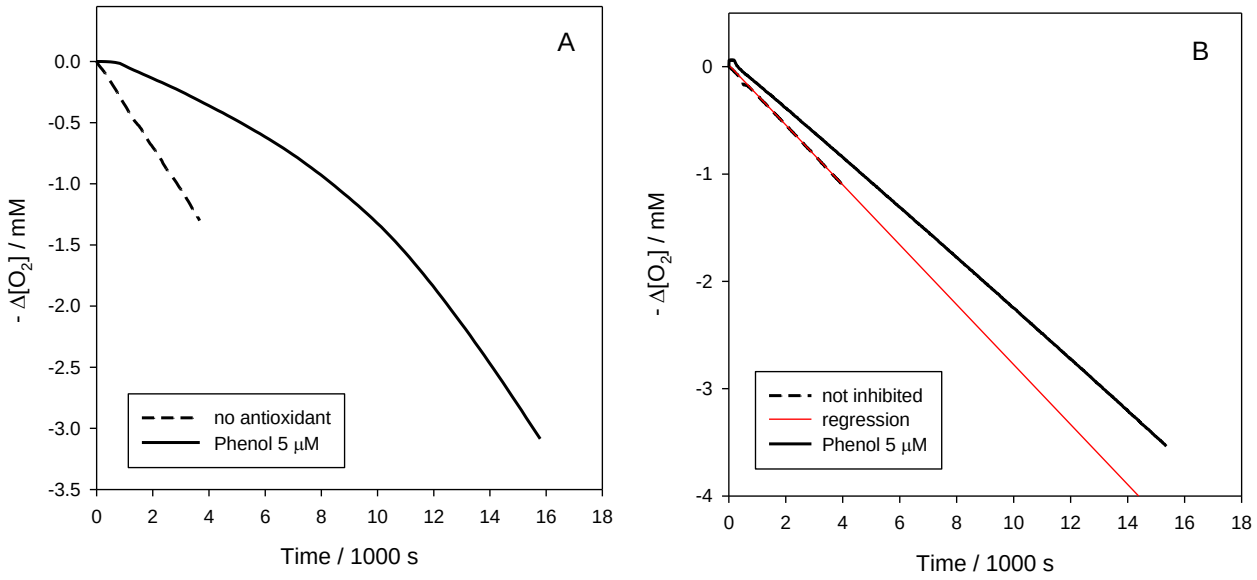

Figure S14. Oxygen consumption during the autoxidation of Cumene (3.6 M) initiated by AIBN (0.05 M) in PhCl (A) or in ACN (B) at 30° C without inhibitors (dashed) or in the presence of 5 μM phenol.

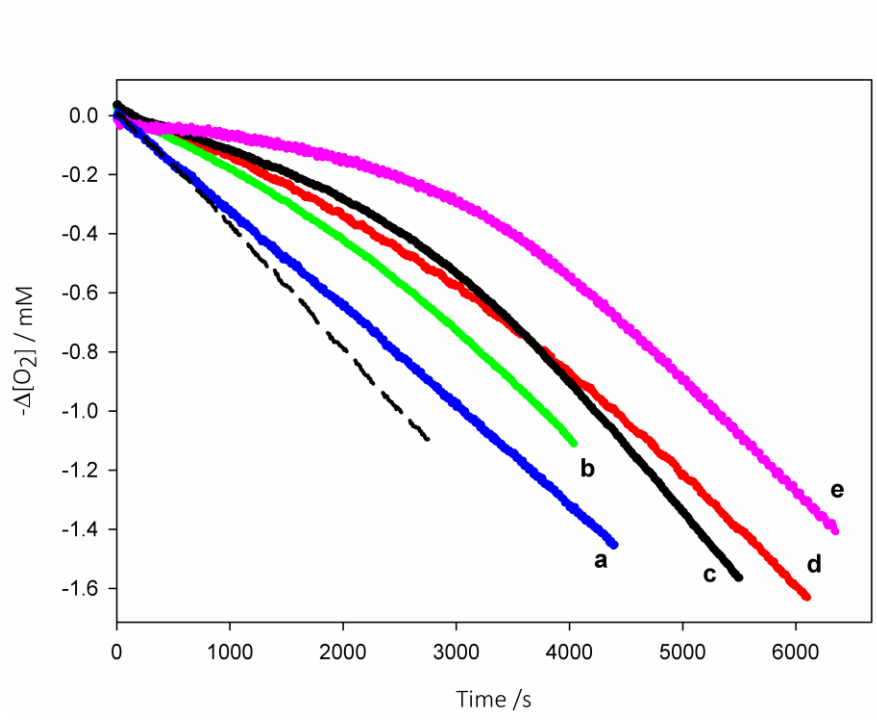

Figure S15. Oxygen consumption during the autoxidation of Cumene (3.6 M) initiated by AIBN (0.05 M) in ACN at 30° C without inhibitors (dashed) or in the presence of the following antioxidants (7.5×10^{-6}M): Umbelliferone (**a**), Thymol (**b**), Eugenol (**c**), Carvacrol (**d**), Coniferyl alcohol (**e**).

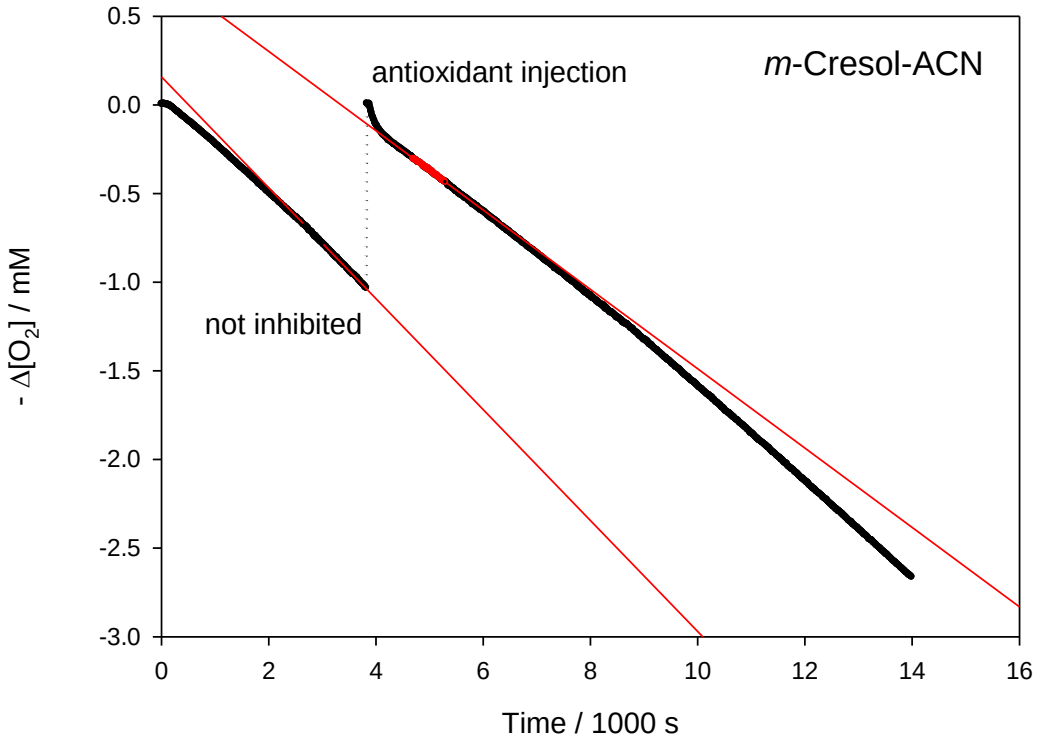

Figure S16. Oxygen consumption during the autoxidation of Cumene (3.6 M) initiated by AIBN (0.05 M) in ACN at 30° C without inhibitors and upon injection of *m*-cresol at a final concentration of 5 µM.

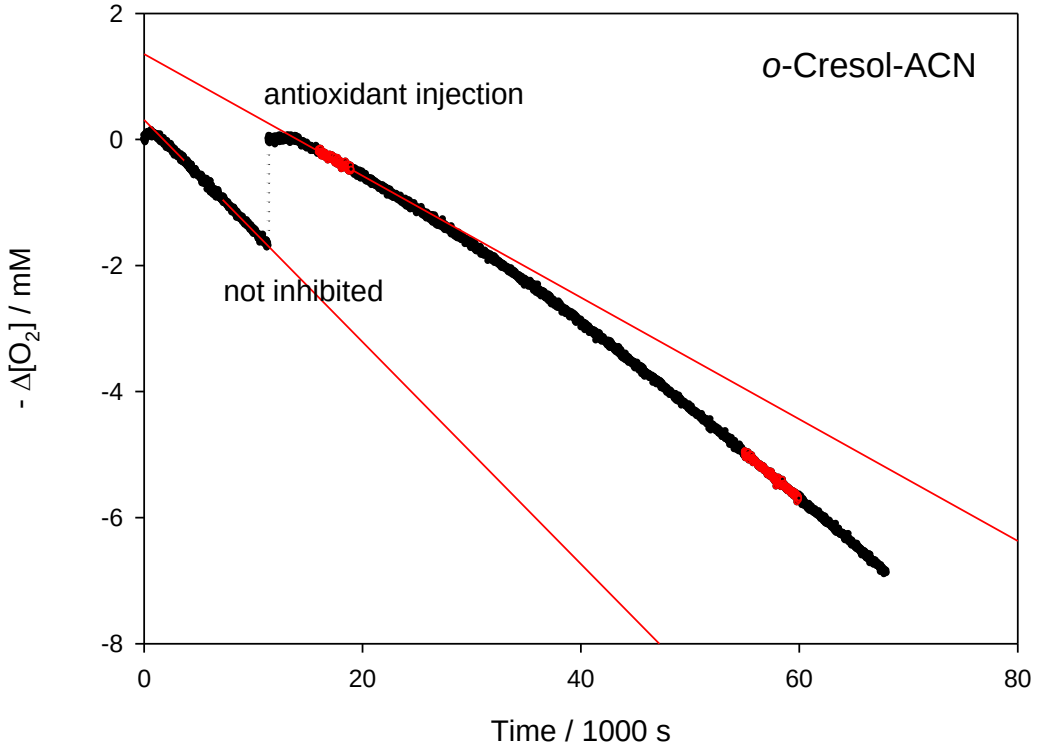

Figure S17. Oxygen consumption during the autoxidation of Cumene (3.6 M) initiated by AIBN (0.05 M) in ACN at 30° C without inhibitors and upon injection of *o*-cresol at a final concentration of 5 µM.

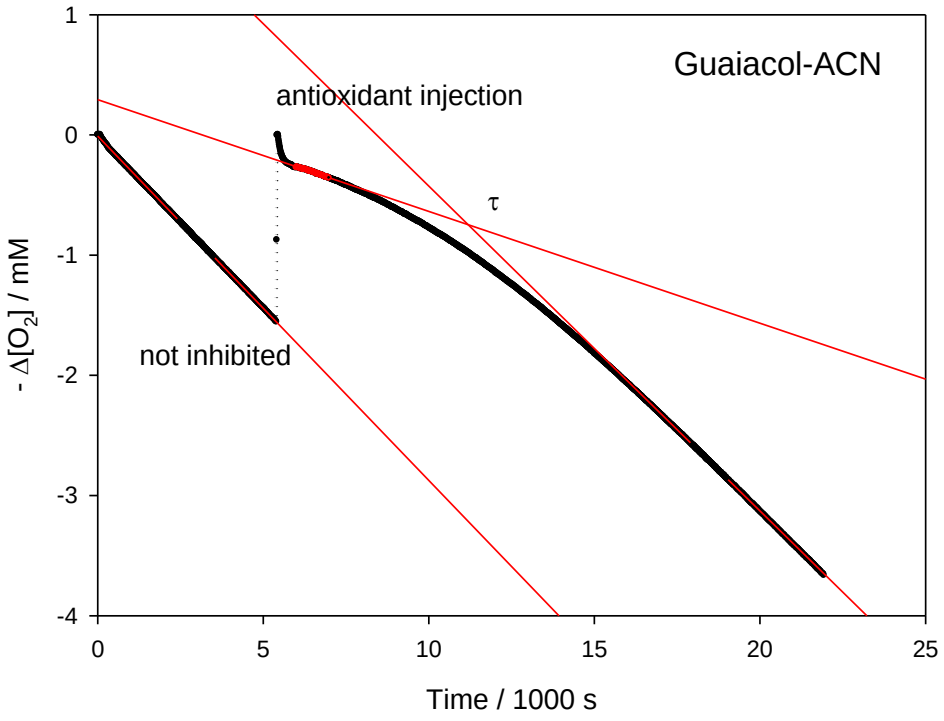

Figure S18. Oxygen consumption during the autoxidation of Cumene (3.6 M) initiated by AIBN (0.05 M) in ACN at 30° C without inhibitors and upon injection of guaiacol at a final concentration of 5 µM.

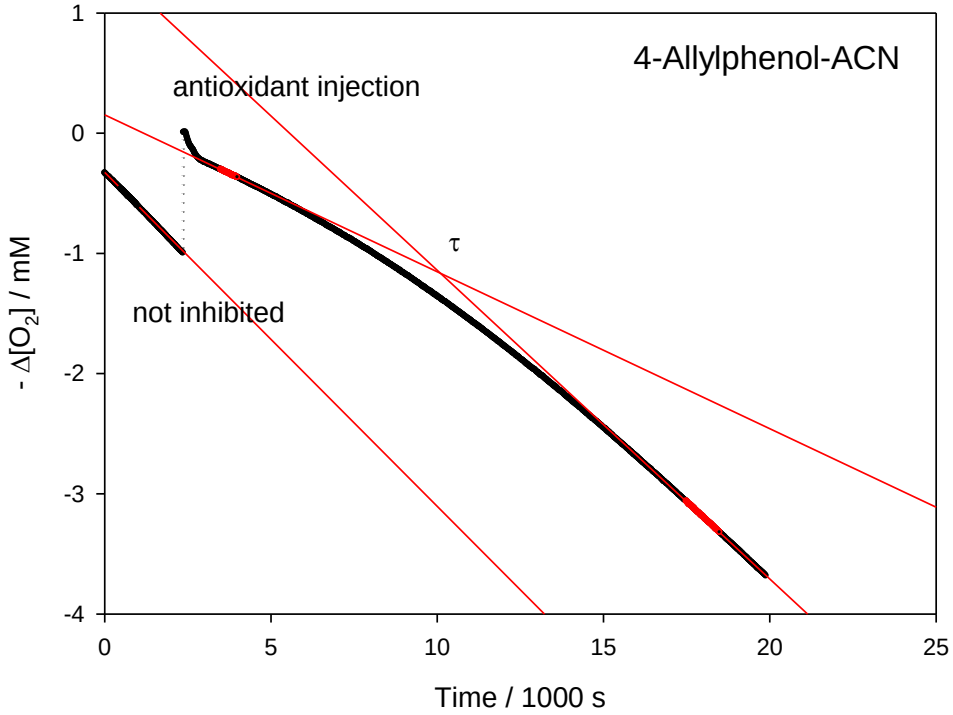

Figure S19. Oxygen consumption during the autoxidation of Cumene (3.6 M) initiated by AIBN (0.05 M) in ACN at 30° C without inhibitors and upon injection of 4-allylphenol at a final concentration of 7 µM.

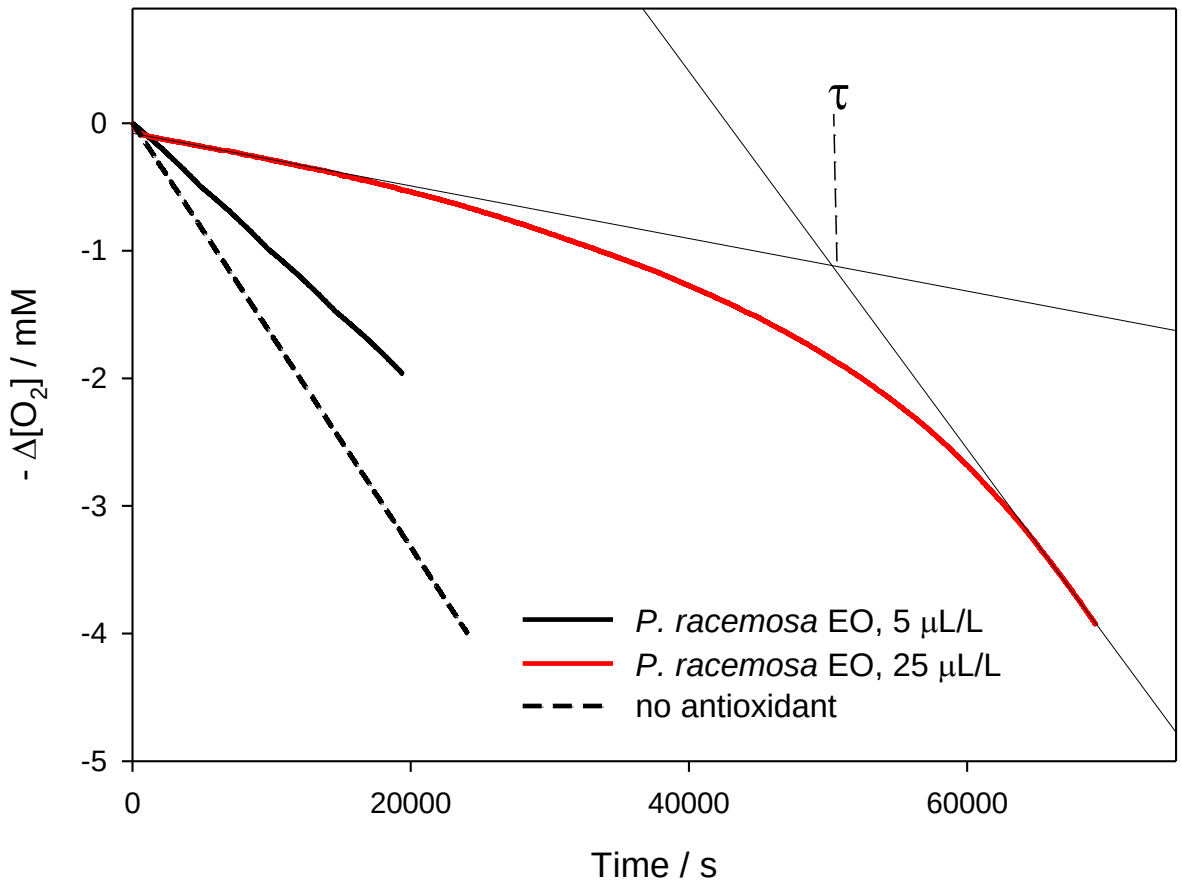

Figure S20. Oxygen consumption during the autoxidation of Olive Oil (50% v/v) in PhCl, initiated by AIBN (0.05 M) at 30° C, without inhibitors and in the presence of Bay St. Thomas (*P. racemosa*) essential oil at different concentrations.

Notes on the kinetic equations (1-3) and their derivation

$$-\frac{d[\mathrm{O_2}]_{inh}}{dt} = \frac{k_p[\mathrm{RH}]R_i}{nk_{inh}[\mathrm{AH}]} \quad (1)$$

$$R_i = \frac{n[\mathrm{AH}]}{\tau} \quad (2)$$

$$\frac{R_0}{R_{inh}} - \frac{R_{inh}}{R_0} = \frac{nk_{inh}[\mathrm{AH}]}{\sqrt{2k_tR_i}} \quad (3)$$

Equations (1)-(3) are not generally valid, but they apply to autoxidations run under controlled conditions, initiated at a constant rate R_i, *e.g.* by the thermal decomposition of a radical initiator.

If the radical initiator is an azo-compounds like AIBN releasing alkyl radicals (and nitrogen gas), the rate of initiation R_i can be defined as the rate of alkyl radical release in the reaction solution following the thermal decomposition of the initiator ($R_i = d[\mathrm{R}\bullet]/dt$; Ms^{-1}), which also accounts for loss of efficiency due to reaction of the initiator's radical fragments in the solvent cage before diffusion into the bulk solution. Since the subsequent transformation of the alkyl radical R• in the peroxyl radical ROO• by reaction with O_2 is very fast and not rate limiting, R_i can also be regarded as the rate of peroxyl radical formation from the initiator ($R_i = d[\mathrm{ROO}\bullet]/dt$; Ms^{-1}).

Equation (1), generally referred to as the Ingold-Howard equation,[S1,S2] is best suited to analyze autoxidation inhibited by a very effective antioxidant AH giving a neat inhibition period, under the assumption that, during such inhibition period, the radical chain is terminated essentially only by the antioxidant, while spontaneous chain termination is negligible. If this assumption cannot be made, then equation (3), often referred to as Denisov's equation,[S3,S4] should be preferred: it is based on comparison of the rate of oxygen uptake in the absence of the inhibitor, R_0, to that recorded in the presence of the inhibitor, R_{inh}.

Both equations provide the rate constant for trapping peroxyl radicals k_{inh} and both require independent determination (or assumption) of the stoichiometric factor n, i.e. the number of peroxyl radicals trapped by one molecule of antioxidant. Both equations also require knowledge of R_i. This can be determined by means of equation (2) from a preliminary set of autoxidations under identical settings as those applied in the subsequent kinetic measurements, using alpha-tocopherol or its synthetic analogue PMHC as the reference antioxidant, since their stochiometric factor $n = 2$ is known from a wealth of studies. This approach is referred to as "the inhibitor method" to measure R_i, and requires the use of a reference antioxidant which would be sufficiently effective to guarantee the approximation that chain termination is caused only by the antioxidant, i.e. every peroxyl radical formed following the decomposition of the radical initiator is quenched by the antioxidant (or its radical) and spontaneous chain termination is negligible. Under such conditions, the length (duration) of the inhibited period τ will be reversely proportional to R_i and directly proportional to the concentration of [AH = PMHC] used in the experiment. Therefore eq. (2) is highly versatile as it can provide any of [AH] or n, or R_i, provided the others are known; however, it should not be overinterpreted as it does not establish a causal relationship between R_i and [AH] or n.

All the above equations can be derived by applying the simple approach of the mass action law and the steady-state approximation of transient species to the simplified reactions' scheme S0-S5

describing the autoxidation radical chain in the absence of an antioxidant AH (reactions S0-S3) or in its presence (S0-S5) using a monophenol as the prototypical antioxidant.

S0) Initiator $\xrightarrow{R_i}$ R$^\bullet$

S1) R$^\bullet$ + O_2 $\xrightarrow{k_1}$ ROO$^\bullet$

S2) ROO$^\bullet$ + RH $\xrightarrow{k_p}$ ROOH + R$^\bullet$

S3) ROO$^\bullet$ + ROO$^\bullet$ $\xrightarrow{k_t}$ Non-radical products

S4) ROO$^\bullet$ + AH $\xrightarrow{k_{inh}}$ ROOH + A$^\bullet$

S5) ROO$^\bullet$ + A$^\bullet$ $\xrightarrow{k_5}$ Non-radical products

Derivation of equations (1) and (2)

The rate of reaction S0 is R_i, while that of S1 is given by

$$-\frac{d[O_2]}{dt} = k_1[R\cdot][O_2] \quad (4)$$

while the rate of transient radical species formation is given by equations (5)-(7)

$$\frac{d[R\cdot]}{dt} = R_i + k_p[ROO\cdot][RH] - k_1[R\cdot][O_2] \quad (5)$$

$$\frac{d[ROO\cdot]}{dt} = k_1[R\cdot][O_2] - 2kt[ROO\cdot]^2 - k_p[ROO\cdot][RH] - k_{inh}[ROO\cdot][AH] - k_5[ROO\cdot][A\cdot] \quad (6)$$

$$\frac{d[A\cdot]}{dt} = k_{inh}[ROO\cdot][AH] - k_5[ROO\cdot][A\cdot] \quad (7)$$

Applying the steady-state approximation for all transient radicals upon onsetting of the radical chain, the expressions (5) and (7) can be set equal to zero, therefore:

$$k_1[R\cdot][O_2] = Ri + k_p[ROO\cdot][RH] \quad (8)$$

$$k_{inh}[ROO\cdot][AH] = k_3[ROO\cdot][A\cdot] \quad (9)$$

Substituting these last two expressions in equation (6) and applying the steady-state approximation for ROO • gives:

$$2k_t[ROO\cdot]^2 + 2k_{inh}[ROO\cdot][AH] - R_i = 0 \quad (10)$$

Solving the equation (10) with respect to [ROO •] and ignoring the negative solution gives:

$$[\mathrm{ROO}\cdot] = \frac{1}{2k_t}\left\{-k_{inh}[\mathrm{AH}] + \sqrt{k_{inh}^2[\mathrm{AH}]^2 + 2k_t R_i}\right\} \quad (11)$$

Substituting equation (8) into (4) affords:

$$-\frac{d[\mathrm{O_2}]}{dt} = k_p[\mathrm{ROO}\cdot][\mathrm{RH}] + R_i \quad (12)$$

Finally, combining (11) and (12) affords (13)

$$-\frac{d[\mathrm{O_2}]}{dt} = \frac{k_p[\mathrm{RH}]}{2k_t}\left\{-k_{inh}[\mathrm{AH}] + \sqrt{k_{inh}^2[\mathrm{AH}]^2 + 2k_t R_i}\right\} + R_i \quad (13)$$

The expression (13) is of a general nature and represents the rate of oxygen consumption during a controlled autoxidation both in the absence and in the presence of an inhibition period, i.e. both in the presence of a weak or a very effective antioxidant. In the latter case it is possible to derive a simpler equation if we consider that, in the presence of a good antioxidant, it is possible to neglect the recombination reaction between two peroxyl radicals (2 ROO• → Products), as the termination reactions with the antioxidant (ROO • + AH) and with the corresponding radical (ROO • + A •) are by far more important. In this case eq (6) becomes:

$$\frac{d[\mathrm{ROO}\cdot]}{dt} = k_1[\mathrm{R}\cdot][\mathrm{O_2}] - k_p[\,\mathrm{ROO}\cdot][\mathrm{RH}] - k_{inh}[\mathrm{ROO}\cdot][\mathrm{AH}] - k_3[\,\mathrm{ROO}\cdot][A\cdot] \quad (14)$$

while equation (10) becomes:

$$2k_{inh}[\mathrm{ROO}\cdot][\mathrm{AH}] - R_i = 0 \quad (15)$$

which can be rewritten as:

$$[\mathrm{ROO}\cdot] = \frac{R_i}{2k_{inh}[\mathrm{AH}]} \quad (16)$$

By substituting equation (16) in (12), the oxygen consumption during the inhibited period will be described by:

$$-\frac{d[\mathrm{O_2}]}{dt} = \frac{k_p[\mathrm{RH}]R_i}{2k_{\mathrm{inh}}[\mathrm{AH}]} + R_i \quad (17)$$

If the chain is long enough, the additive term R_i can be neglected to afford equation (1a), for an antioxidant having a stoichiometric factor $n = 2$.

$$-\frac{d[O_2]}{dt} = \frac{k_p[RH]R_i}{2k_{inh}[AH]} \quad (1a)$$

During such inhibition the concentration of the antioxidant will decrease according to eq. (18)

$$-\frac{d[AH]}{dt} = k_{inh}[AH][ROO\cdot] \quad (18)$$

Substituting in equation (18) the equation (16) gives:

$$-\frac{d[AH]}{dt} = \frac{R_i}{2} \quad (19)$$

Integrating the differential equation between time 0 and any time t gives:

$$-\int_0^t d[AH] = \frac{R_i}{2}\int_0^t dt \quad (20)$$

$$[AH]_0 - [AH]t = \frac{R_i}{2}t \quad (21)$$

By choosing t = τ, that is the time at which all the inhibitor has been consumed we obtain:

$$[AH]_0 = \frac{Ri}{2}\tau \quad (22)$$

which can be rewritten as equation (2a) for an antioxidant trapping *n* =2 radicals

$$R_i = \frac{2[AH]_0}{\tau} \quad (2a)$$

The term 2 that appears both in eq (1a) and (2a) is the stoichiometric coefficient *n*, which in general can assume values different from 2. It is therefore possible, to write the same equations in a more general form, using the term *n* in place of 2, to afford the general expressions (1) and (2).

It should be noted that equation (13) is also generally valid in the absence on an antioxidant, by setting [AH]=0. On doing so, it can be simplified to equation (23) describing the rate of an uninhibited autoxidation initiated at constant rate by an azo initiator:

$$-\frac{d[O_2]}{dt} = \frac{k_p}{\sqrt{2k_t}}[RH]\sqrt{R_i} + R_i \quad (23)$$

If the chain length is sufficiently long (>20) the expression can be simplified by omitting the additive term R_i, as:

$$-\frac{d[O_2]}{dt} = \frac{k_p}{\sqrt{2k_t}}[RH]\sqrt{R_i} \quad (24)$$

Derivation of equation (3)

The rate of an uninhibited autoxidation, from now on indicated as R_0, is given by equation (24), which can be rewritten as:

$$R_0 = k_p[\mathrm{RH}](R_i/2k_t)^{1/2} \qquad (24a)$$

On the other hand, the rate of an inhibited autoxidation, from now on indicated as R_{inh} can be indicated as:

$$R_{inh} = k_p[\mathrm{RH}][\mathrm{ROO}\cdot] \qquad (25)$$

with the understanding that the concentration [ROO·] is the steady state-state concentration in the presence of the antioxidant, given by equation (11). Therefore, the ratio R_{inh}/R_0 is given by:

$$R_{inh}/R_0 = [\mathrm{ROO}\cdot](2k_t/R_i)^{1/2} \qquad (26)$$

The concentration of [ROO·] arising from it is:

$$[\mathrm{ROO}\cdot] = \frac{R_{inh}}{R_0}(R_i/2k_t)^{1/2} \qquad (26a)$$

The rate of peroxyl radical formation during the autoxidation is given by equation (6), which can be rewritten as (27) considering that, for most antioxidants trapping more than one radical, reaction S4 is rate limiting over S5, *i.e.* the subsequent trapping is much faster than the first (*n* represents the general stoichiometric factor).

$$\frac{d[\mathrm{ROO}\cdot]}{dt} = k_1[\mathrm{R}\cdot][\mathrm{O_2}] - 2kt[\mathrm{ROO}\cdot]^2 - k_p[\mathrm{ROO}\cdot][\mathrm{RH}] - nk_{inh}[\mathrm{ROO}\cdot][\mathrm{AH}] = 0 \qquad (27)$$

Substituting equation (8) into equation (27) affords:

$$R_i + k_p[\mathrm{ROO}\cdot][\mathrm{RH}] - 2kt[\mathrm{ROO}\cdot]^2 - k_p[\mathrm{ROO}\cdot][\mathrm{RH}] - nk_{inh}[\mathrm{ROO}\cdot][\mathrm{AH}] = 0$$

which simplifies to equation (28).

$$R_i - 2kt[\mathrm{ROO}\cdot]^2 - nk_{inh}[\mathrm{ROO}\cdot][\mathrm{AH}] = 0 \qquad (28)$$

Substitution of (26a) into equation (28) and simplification affords:

$$R_i - (\frac{R_{inh}}{R_0})^2 R_i - nk_{inh}[\mathrm{AH}]\frac{R_{inh}}{R_0}(R_i/2k_t)^{1/2} = 0 \qquad (29)$$

Dividing both terms by R_i, then by R_{inh}/R_0 affords the equivalent expression:

$$\frac{R_0}{R_{inh}} - \frac{R_{inh}}{R_0} - \frac{nk_{inh}[\mathrm{AH}]}{\sqrt{(2k_tR_i)}} = 0 \qquad (3a)$$

which can easily be rearranged to equation (3)

References

S1) Howard, J.A. In: Free Radicals; Kochi, J.K. (Ed.); Wiley, New York, 1973; vol 2, Chapter 12,

S2) Burton, G.W.; Ingold, K.U. Autoxidation of Biological Molecules. 1. The Antioxidant Activity of Vitamin E and Related Chain-Breaking Phenolic Antioxidants in Vitro. *J. Am. Chem. Soc.* **1981**, *103*, 6472-6477.

S3) Denisov, E.T.; Khudyakov, I.V. Mechanisms of Action and Reactivities of the Free Radicals of Inhibitors. *Chem. Rev.* **1987**, *87*, 1313-1357.

S4) Denisov, E. T. Elementary Reactions of Oxidation Inhibitors. *Russ. Chem. Rev.* **1973**, *42*, 157-172.